NUKLEONIKA 2015;60(3):411–416
doi: 10.1515/nuka-2015-0073

ORIGINAL PAPER

DE GRUYTER
OPEN

Magnetic resonance study of co-modified (Co,N)-TiO_2 nanocomposites

Niko Guskos,
Grzegorz Zolnierkiewicz,
Aleksander Guskos,
Janusz Typek,
Pawel Berczynski,
Diana Dolat,
Sylwia Mozia,
Constantinos Aidinis,
Antoni W. Morawski

Abstract. Three nCo,N-TiO_2 nanocomposites (where cobalt concentration index n = 1, 5 and 10 wt%) were prepared and investigated by magnetic resonance spectroscopy at room temperature. Ferromagnetic resonance (FMR) lines of magnetic cobalt agglomerated nanoparticle were dominant in all registered spectra. The relaxation processes and magnetic anisotropy of the investigated spin system essentially depended on the concentration of cobalt ions. It is suggested that the samples contained two magnetic types of sublattices forming a strongly correlated spin system. It is suggested that the existence of strongly correlated magnetic system has an essential influence of the photocatalytic properties of the studied nanocomposites.

Key words: nanocomposites • titanium dioxide • ferromagnetic resonance

N. Guskos
Department of Solid State Physics,
Faculty of Physics,
University of Athens,
Panepistimioupolis, GR-157 84 Athens, Greece
and Department of Physics,
West Pomeranian University of Technology,
48 Piastow Ave., 70-311 Szczecin, Poland

G. Zolnierkiewicz✉, A. Guskos, J. Typek, P. Berczynski
Department of Physics,
West Pomeranian University of Technology,
48 Piastow Ave., 70-311 Szczecin, Poland,
Tel.: +48 91 449 4595, Fax: +48 91 449 4181,
E-mail: gzolnierkiewicz@zut.edu.pl

D. Dolat, S. Mozia, A. W. Morawski
Institute of Chemical and Environmental Engineering,
West Pomeranian University of Technology,
10 Pulaskiego Str., 70-322 Szczecin, Poland

C. Aidinis
Department of Electronics-Computers-
-Telecommunications and Control,
Faculty of Physics,
University of Athens,
Panepistimioupolis, GR-157 84 Athens, Greece

Received: 7 October 2014
Accepted: 30 January 2015

Introduction

Many papers have been recently published devoted to the magnetic atoms (from 3D transition group) – modified titanium dioxide that concerned their magnetic and photocatalytic properties, e.g. [1–17]. Observed long-range magnetic interaction in these materials gives rise to ferromagnetic ordering at room temperature and is related to semiconductor's properties which are very interesting and could find application in the so-called spintronics. It has also been shown that some ions from the transition metal group improve the photocatalytic properties [18, 19]. Experiments have clearly demonstrated the occurrence of magnetic order at room temperature in titanium dioxide modified by cobalt. Unfortunately, the mechanism responsible for this state is not yet fully understood. The resulting oxygen vacancies associated with the presence of titanium ions in lower oxidation state [19] could be involved in the formation of ferromagnetic state. The method of sample preparation significantly affects its physical properties. Localized magnetic moments of the agglomerates and their concentration have a dominant influence on these properties and ferromagnetic resonance (FMR)/electron paramagnetic resonance (EPR) spectroscopy could help to understand magnetic interactions [19–30]. In previous work investigation of the temperature dependence of the FMR/EPR spectra of co-modified systems nM,N-TiO_2 (where n = 1, 5, 10 wt%, M = Fe, Ni) has been carried out [19, 30]. Measurements have shown that these are complex magnetic systems and thus improved understanding of their magnetism requires further investigations that in turn will optimize and expand their potential applications.

The aim of this work was to study the static FMR spectra of three co-modified nCo,N-TiO_2 (n = 1, 5, 10 wt% of Co) nanopowders at room temperature (RT). As the magnetic interactions of agglomerates have an influence on their photocatalytic activity, the investigation of the magnetic properties of nCo,N-TiO_2 could help to gain knowledge of the mechanisms responsible for the extended applications of titanium dioxide.

Experimental

Amorphous titanium dioxide (TiO_2/A) from the sulfate technology supplied by Chemical Factory Police S.A. (Poland) was used as a starting material for the synthesis of the (Co,N) – co-modified rutile TiO_2 photocatalysts, as previously described [31]. A fixed amount of TiO_2 water suspension was stirred for 48 h in a beaker with an appropriate amount of $Co(NO_3)_2 \cdot 5H_2O$ such that the amount of Co introduced to the beaker was of 1, 5, or 10 wt% relatively to TiO_2 content. Subsequently, samples were dried at 80°C for 24 h in an oven and annealed at 800°C in a NH_3 flow. The obtained samples will be designated further as 1Co,N, 5Co,N, and 10Co,N.

X-ray diffraction (XRD) measurements of the synthesized samples have shown mainly the presence of TiO_2 rutile phase and small amounts of cobalt which increased with an increase in index n. X-ray photoelectron spectroscopy (XPS) has shown that the cobalt ions are on the second level of oxidation. Measurements of magnetic resonance spectra were performed on a conventional X-band (ν = 9.4 GHz) Bruker E 500 spectrometer with a 100 kHz magnetic field modulation. The measurements were performed at room temperature. Photocatalytic activity of samples was evaluated on the basis of decomposition of acetic acid (AcOH) in aqueous solutions in ambient air. 400 W high-pressure mercury lamp (Eiko-sha, Japan) with a cut-off filter providing irradiation of wavelength greater than 400 nm was used as a source of solar light irradiation. All the conditions were the same as described in previous publication [31]. All materials showed moderate photocatalytic activity, the lowest photocatalytic performance was obtained for 5Co, N nanocomposite (see Fig. 1).

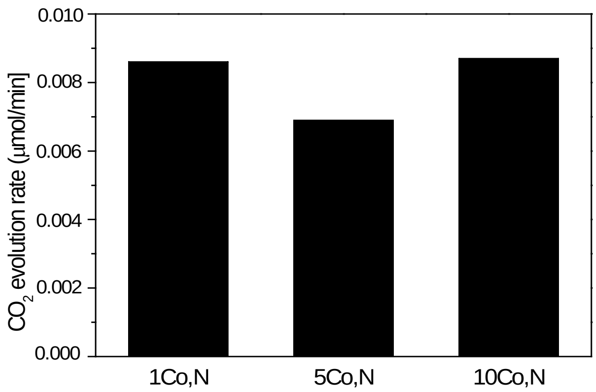

Fig. 1. CO_2 photocatalytic evolution during acetic acid decomposition under mercury lamp irradiation, combined with a cut-off filter (>400 nm) in the presence of nCo,N nanocomposites (n = 1, 5, 10).

Results and discussion

XRD measurements for the investigated nanocomposites are shown in Fig. 2. XRD analysis confirmed the complete transformation of anatase and amorphous phase to rutile. For all samples, no nitrogen was detected. This may be attributed to the fact that at this high cobalt concentration, cobalt species clog up the pores in titanium dioxide preventing nitrogen incorporation. For samples 5Co,N and 10Co,N, cobalt residues were recorded.

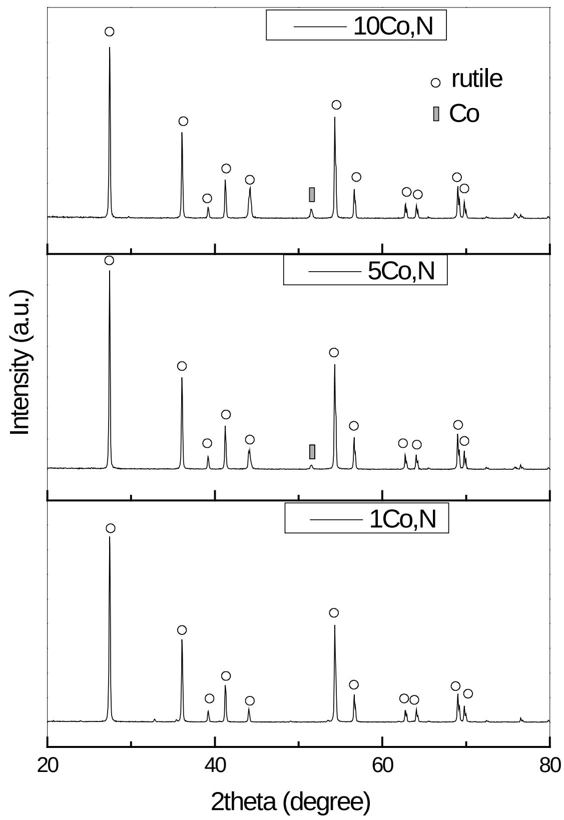

Fig. 2. XRD patterns of nCo,N nanocomposites (n = 1, 5, 10).

Table 1. Quantitative composition of the nanocomposites surface from XPS study

Sample	Ti [wt%]	O [wt%]	C [wt%]	Co [wt%]
1Co,N	12.5	43.6	43.9	–
5Co,N	11.5	50.8	29.2	8.4
10Co,N	13.9	51.1	27.8	7.2

XPS measurements of quantitative composition of the surface are shown in Table 1. In none of the samples was nitrogen detected, which may mean that its concentration at the samples surface was below the detection level of at 1%. High intensity of the satellite structure in the spectrum indicates the presence of cobalt element on the oxidation state +2. The 5Co,N and 10Co,N samples have a lower ratio of O/Ti. Because this ratio value is approx. 3 or more, it is suggested that the surface is constructed from the phases between the $Ti(OH)_4$ and $TiO(OH)_2$.

In order to confirm presence of nitrogen in the studied materials, elemental analysis was carried out. As shown in Table 2 materials with 5 and 10% of Co do not contain nitrogen, which was only detected in small amounts in the sample prepared with 1% of Co.

The UV-Vis/DR spectra for (Co,N)-co-modified samples are shown in Fig. 3. All studied materials exhibit good visible light absorption, as in the case of (Fe,N)-TiO_2-co-modified [18].

Table 2. Elemental analysis of nitrogen in all investigated samples

Sample	Nitrogen concentration [wt%]
1Co,N	0.75
5Co,N	0
10Co,N	0

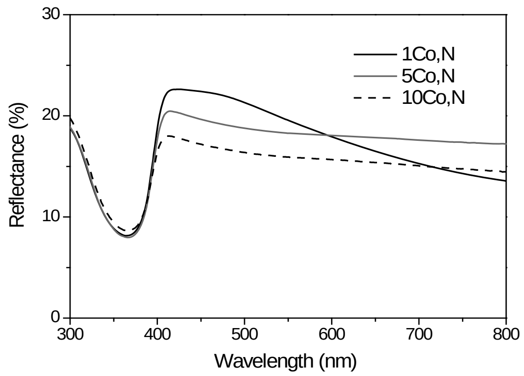

Fig. 3. UV-Vis/DR spectra of nCo,N nanocomposites (n = 1, 5, 10).

EPR/FMR spectra of the three investigated samples at room temperature (RT) are shown in Fig. 4. The experimental resonance spectra (empty squares) are dominated by a single, intense, broad and strongly asymmetrical line for all samples that are typical for strong magnetic interactions of metal or metal oxide nanoparticle agglomerates [32–34]. With the increase of cobalt concentration, this interaction gets stronger.

The FMR spectra of nCo,N samples were satisfactory fitted by using four spectral components of the Callen lineshape. These components represent, in a very simplified way, lines that are produced by magnetic anisotropy of the spin system. The following equation for the Callen lineshape is obtained in a case of the linear polarization of the microwave field [34, 35]:

$$(1)\qquad I(H) \propto \frac{H_r^2\left[\begin{aligned}&\left(H_r^2+\Delta_H^2\right)\left(H^2\Delta_H+2H_r|H|\delta_H\right)\\&+H_r^2\left(H_r^2+\delta_H^2\right)\Delta_H\end{aligned}\right]}{\begin{aligned}&\left[\left(H-H_r\right)^2H_r^2+\left(|H|\Delta_H+H_r\delta_H\right)^2\right]\\&\cdot\left[\left(H+H_r\right)^2H_r^2+\left(|H|\Delta_H+H_r\delta_H\right)^2\right]\end{aligned}}$$

where H_r is the resonance field, Δ_H is the linewidth connected with relaxation of the Landau–Lifshitz type, and δ_H the linewidth connected with the Bloch–Bloembergen relaxation. Under certain circumstances, the Landau–Lifshitz relaxation can be identified with the longitudinal (spin-lattice) and the Bloch–Bloembergen with the transverse (spin-spin) relaxations.

Results of fitting (solid lines) are shown in Fig. 4. All parameters in Eq. (1) strongly depended on the concentration of cobalt (see Tables 3–6). It could be suggested that, inside the samples, two magnetic sublattices could form and essentially interact with each another. The resonance fields displayed essential differences for samples with different cobalt concentration (Table 3). These four components could be paired in two magnetic systems: I and II. Assuming that the overall magnetic anisotropy field H_{anis} scales with the difference in magnetic fields of the components, H_{anis}

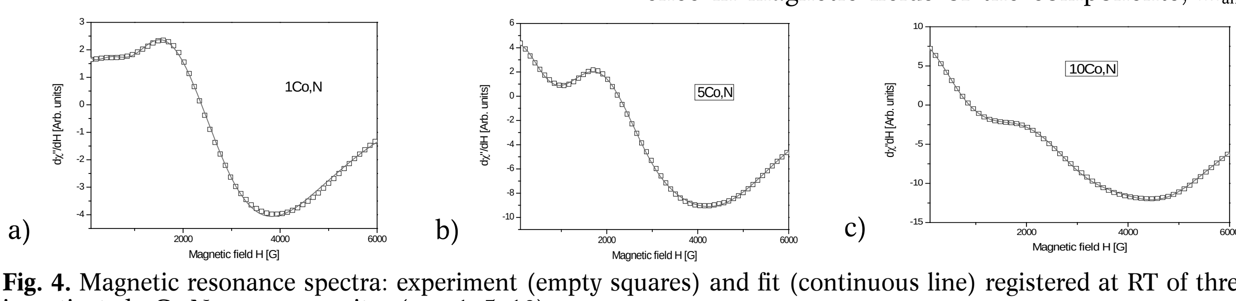

Fig. 4. Magnetic resonance spectra: experiment (empty squares) and fit (continuous line) registered at RT of three investigated nCo,N nanocomposites (n = 1, 5, 10).

Table 3. Values of the resonance fields H_r obtained from fittings

Sample	$H_r(1)$ [G]	$H_r(2)$ [G]	$H_r(3)$ [G]	$H_r(4)$ [G]
1Co,N	3416(30)	1700(30)	1300(30)	10 000(70)
5Co,N	4247(40)	2020(60)	5200(50)	12 800(90)
10Co,N	4158(50)	2540(40)	4900(70)	10 800(90)

Table 4. Values of the linewidths Δ_H obtained from fittings

Sample	$\Delta_H(1)$ [G]	$\Delta_H(2)$ [G]	$\Delta_H(3)$ [G]	$\Delta_H(4)$ [G]
1Co,N	1300(50)	2500(40)	~0	900(90)
5Co,N	3450(40)	2070(30)	2800(90)	1600(20)
10Co,N	2700(30)	2500(40)	2000(10)	~0

Table 5. Values of linewidths Δ_H obtained from fittings

Sample	$\Delta_H(1)$ [G]	$\Delta_H(2)$ [G]	$\Delta_H(3)$ [G]	$\Delta_H(4)$ [G]
1Co,N	1800(20)	2600(40)	14 200(90)	390(90)
5Co,N	300(50)	1400(20)	~0	14 400(80)
10Co,N	700(70)	2000(10)	~0	14 400(80)

Table 6. Amplitudes and integrated intensities of components obtained from fittings

Sample	$A(1)$ [a.u.]	$A(2)$ [a.u.]	$A(3)$ [a.u.]	$A(4)$ [a.u.]	I/I_1	$I(\Delta)/I_1(\Delta)$	$I(\delta)/I_1(\delta)$
1Co,N	1.3	0.65	8.20	0.022	1.0	1.0	1.0
5Co,N	1.5	0.86	0.44	16	1.9	0.8	2.9
10Co,N	1.9	2.5	0.28	19	2.4	1.5	2.7

$\sim H_i - H_j$, the largest H_{anis} fields are calculated for sample 1Co,N (H_{anis}(I) ~ 1.7 kG and H_{anis}(II) ~ 8.7 kG), next for sample 5Co,N (H_{anis}(I) ~ 1.8 kG and H_{anis}(II) ~ 7.6 kG) and the smallest for sample 10Co,N (H_{anis}(I) ~ 1.6 kG and H_{anis}(II) ~ 5.9 kG). In the case of system I of magnetic agglomerates, the magnetic anisotropy did not vary significantly in the three samples, but in the second system (designated as II), it decreased with increased concentration of cobalt. Overall, the magnetic anisotropy in the present samples is smaller than that in co-modified nFe,N-TiO_2 nanocomposites [19].

The linewidth connected with the relaxation of the Landau–Lifshitz type Δ_H is the biggest for sample 5Co,N and the smallest for sample 1Co,N (see Table 4). On the other hand, the linewidth connected with the Bloch–Bloembergen relaxation δ_H is the biggest for samples 1Co,N and the smallest for samples 10Co,N (see Table 5). The amplitudes and relative integrated intensities are shown in Table 6. The FMR integrated intensity, calculated as the product of the amplitude and the linewidth squared, is assumed to reflect the concentration of nanoparticles. Both the amplitude and the integrated intensity increased with increased concentration of cobalt ions. Dipole interactions affecting the width of the line do not necessarily increase with an increasing concentration of magnetic centers. The reason for this lies with the processes of reorientation of correlated spin systems. Table 6 also shows separate relative integrated intensities for different relaxation processes. A significant jump in relative intensities observed when moving from sample 1Co,N and 5Co,N concerning the process of the Bloch–Bloembergen relaxation is easily to observe.

Photocatalytic activity of the investigated samples is not as good as for previously studied co-modified nFe,N-TiO_2 nanocomposites [18]. It is likely that the presence of $FeTiO_3$ phase and doped nitrogen in TiO_2 structure improves its photocatalytic performance under visible light irradiation. On the other hand, the presence of two different magnetic sublattices may significantly affect the various physicochemical properties of nCo,N-TiO_2 nanocomposites.

Conclusions

The FMR spectra of co-modified nCo,N-TiO_2 samples have shown the occurrence of strongly coupled spin systems of two types. Relaxation processes and magnetic anisotropies quite significantly depended on cobalt concentration. The increase in concentration of correlated systems differently affects the resonance fields and dipole-dipole interactions. It has been suggested that the presence of two magnetic sublattices adversely affect the photocatalytic performance.

Acknowledgment. This work was partially supported by the National Centre for Science and Ministry of Science and Higher Education of Poland under project no. MNiSW/DPN/4878/TD/2010, Decision no. 802/N-JAPONIA/2010/O.

References

1. Kim, D. H., Yang, J. S., Lee, K. W., Bu, S. D., Noh, T. W., Oh, S. -J., Kim, Y. -W., Chung, J. -S., Tanaka, H., Lee, H. Y., & Kawai, T. (2002). Formation of Co nanoclusters in epitaxial $Ti_{0.96}Co_{0.04}O_2$ thin films and their ferromagnetism. *Appl. Phys. Lett.*, *81*, 2421–2423.
2. Punnoose, A., Seehra, M. S., Park, W. K., & Moodera, J. S. (2003). On the room temperature ferromagnetism in Co-doped TiO_2 films. *J. Appl. Phys.*, *93*, 7867–7869.
3. Santara, B., Pal, B., & Giri, P. K. (2011). Signature of strong ferromagnetism and optical properties of Co doped TiO_2 nanoparticles. *J. Appl. Phys.*, *110*, 114322.
4. Hong, N. H., Sakai, J., Prellier, W., Hassini, A., Ruyter, A., & Gervais, F. (2004). Ferromagnetism in

transition-metal-doped TiO_2 thin films. *Phys. Rev. B*, *70*, 195204.

5. Griffin, K. A., Pakhomov, A. B., Wang, C. M., Heald, S. M., & Krishnan Kannan, M. (2005). Intrinsic ferromagnetism in insulating cobalt doped anatase TiO_2. *Phys. Rev. Lett*., *94*, 157204.
6. Sangaletti, L., Mozzati, M. C., Galinetto, P., Azzoni, C. B., Speghini, A., Bettinelli, M., & Calestani, G. (2006). Ferromagnetism on a paramagnetic host background: the case of rutile TM:TiO_2 single crystals (TM = Cr, Mn, Fe, Co, Ni, Cu). *J. Phys.-Condens. Matter*, *18*, 7643–7650.
7. Nefedov, A., Akdogan, N., Zabel, H., Khaibullin, R. I., & Tagirov, L. R. (2006). Spin polarization of oxygen atoms in ferromagnetic Co-doped rutile TiO_2. *Appl. Phys. Lett*., *89*, 182509.
8. Park, Y. R., Choi, S., Lee, J. H., Kim, K. J., & Kim, C. S. (2007). Ferromagnetic properties of Ni-doped rutile $TiO_{2-\delta}$. *J. Korean Phys. Soc*., *50*, 638–642.
9. Kim, D., Hong, J., Park, Y. R., & Kim, K. J., (2009). The origin of oxygen vacancy induced ferromagnetism in undoped TiO_2. *J. Phys.-Condens. Matter*, *21*, 195405(4pp.).
10. Li, H., Liu, M., Zeng, Y., & Huang, T. (2010). Coexistence of antiferromagnetic and ferromagnetic in Mn-doped anatase TiO_2 nanowires. *J. Cent. South Univ.*, *17*, 239–243.
11. Green, I. X., Tang, W., Neurock, M., & Yates, J. T. Jr (2011). Spectroscopic observation of dual catalytic sites during oxidation of CO on a Au/TiO_2 catalyst. *Science*, *333*, 736–739.
12. Mudarra Navarro, A. M., Bilovol, V., Cabrera, A. F., & Rodriguez Torres, C. E. (2012). Relationship between structural and magnetic properties in (Ti,Fe) O_2 powders obtained by mechanical milling. *Physica B*, *407*, 3225–3228.
13. Zhao, Y. L., Motapothula, M., Yakovlev, N. L., Liu, Z. Q., Dhar, S., Rusydi, A., Ariando, Breese, M. B. H., Wang, Q., & Venkatesan, T. (2012). Reversible ferromagnetism in rutile TiO_2 single crystals induced by nickel impurities. *Appl. Phys. Lett*., *101*, 142105.
14. Parras, M., Varela, A., Cortes-Gil, R., Boulahya, K., Hernando, A., & Gonzales-Calbet, J. M. (2013). Room-temperature ferromagnetism in reduced rutile $TiO_{2-\delta}$ nanoparticles. *J. Phys. Chem. Lett*., *4*, 2171–2176.
15. Nakai, I., Sasano, M., Inui, K., Korekawa, T., Ishijima, H., Katoh, H., Li, Y. J., & Kurisu, M. (2013). Oxygen vacancy and magnetism of a room temperature ferromagnet Co-doped TiO_2. *J. Korean Phys. Soc*., *63*, 532–537.
16. Choudhury, B., & Choudhury, A. (2013). Structural, optical and ferromagnetic properties of Cr doped TiO_2 nanoparticles. *Mater. Sci. Eng. B*, *178*, 794–800.
17. Santara, B., Giri, P. K., Dhara, S., Imakita, K., & Fuji, M. (2014). Oxygen vacancy-mediated enhanced ferromagnetism in undoped and Fe-doped TiO_2 nanoribbons. *J. Phys. D-Appl. Phys*., *47*, 235304(14pp.).
18. Dolat, D., Mozia, S., Ohtani, B., & Morawski, A. W. (2013). Nitrogen, iron-single modified (N-TiO_2, Fe-TiO_2) and co-modified (Fe,N-TiO_2) rutile titanium dioxide as visible-light active photocatalysts. *Chem. Eng. J*., *225*, 358–364.
19. Guskos, N., Glenis, S., Zolnierkiewicz, G., Guskos, A., Typek, J., Berczynski, P., Dolat, D., Grzmil, B., Ohtani, B., & Morawski, A. W. (2014). Magnetic resonance study of co-modified (Fe,N)-TiO_2. *J. Alloy. Compd.*, *606*, 32–36.
20. Coronado, J. M., Maira, A. J., Conesa, J. C., Yeung, K. L., Augugliaro, V., & Soria, J. (2001). EPR study of the surface characteristics of nanostructured TiO_2 under UV irradiation. *Langmuir*, *17*, 5368–5374.
21. Mele, G., Del Sole, R., Vasapollo, G., Marci, G., Garcia-Lopez, E., Palmisano, L., Coronado, J. M., Hernandez-Alonso, M. D., Malitesta, C., & Guascito, M. R. (2005). TRMC, XPS, and EPR characterizations of polycrystalline TiO_2 porphyrin impregnated powders and their catalytic activity for 4-nitrophenol photodegradation in aqueous suspension. *J. Phys. Chem. B*, *109*, 12347–12352.
22. Yang, S., Halliburton, L. E., Manivannan, A., Bunton, P. H., Baker, D. B., Klemm, M., Horn, S., & Fujishima, A. (2009). Photoinduced electron paramagnetic resonance study of electron traps in TiO_2 crystals: Oxygen vacancies and Ti^{3+} ions. *Appl. Phys. Lett*., *94*, 162114(3pp.).
23. Tian, B., Li, C., Gu, F., Jiang, H., Hu, Y., & Zhang, J. (2009). Flame sprayed V-doped TiO_2 nanoparticles with enhanced photocatalytic activity under visible light irradiation. *Chem. Eng. J*., *151*, 220–227.
24. Brandao, F. D., Pinheiro, M. V. B., Ribeiro, G. M., Medeiros-Ribeiro, G., & Krambrock, K. (2009). Identification of two light-induced charge states of the oxygen vacancy in single-crystalline rutile TiO_2. *Phys. Rev. B*, *80*, 235204.
25. Yang, S., Brant, A. T., & Halliburton, L. E. (2010). Photoinduced self-trapped hole center in TiO_2 crystals. *Phys. Rev. B*, *82*, 035209.
26. Macdonald, I. R., Howe, R. F., Zhang, X., & Zhou, W. (2010). *In situ* EPR studies of electron trapping in a nanocrystalline rutile. *J. Photochem. Photobiol. A-Chem*., *216*, 238–243.
27. Shkrob, I. A., Marin, T. W., Chemerisov, S. D., & Sewilla, M. D. (2011). Mechanistic aspects of photooxidation of polyhydroxylated molecules on metal oxides. *J. Phys. Chem. C*, *115*, 4642–4648.
28. Guskos, N., Guskos, A., Typek, J., Berczynski, P., Dolat, D., Grzmil, B., & Morawski, A. (2012). Influence of annealing and rinsing on magnetic and photocatalytic properties of TiO_2. *Mater. Sci. Eng. B*, *177*, 223–227.
29. Guskos, N., Typek, J., Guskos, A., Berczynski, P., Dolat, D., Grzmil, B., & Morawski, A. (2013). Magnetic resonance study of annealed and rinsed N-doped TiO_2 nanoparticles. *Cent. Eur. J. Chem*., *11*, 1996–2004.
30. Guskos, N., Zolnierkiewicz, G., Guskos, A., Typek, J., Berczynski, P., Dolat, D., Mozia, S., & Morawski, A. W. (2015). Magnetic resonance study of nickel and nitrogen co-modified titanium dioxide nanocomposites. In *NATO Science for Peace and Security Series – C: Environmental Security, "Nanotechnology in the security systems", 29 September – 3 October 2013* (pp. 33–48). Dordrecht: Springer.
31. Dolat, D., Mozia, S., Wrobel, R. J., Moszynski, D., Ohtani, B., Guskos, N., & Morawski, A. W. (2015). Nitrogen-doped, metal-modified rutile titanium dioxide as photocatalysts for water remediation. *Appl. Catal. B-Environ*., *162*, 310–318.
32. Guskos, N., Anagnostakis, E. A., Gasiorek, G., Typek, J., Bodziony, T., Narkiewicz, U., Arabczyk, W., & Konicki, W. (2004). Magnetic resonance study of α-Fe and Fe_3C nanoparticle agglomerates in a nonmagnetic matrix. *Mol. Phys. Rep*., *39*, 58–65.
33. Guskos, N., Typek, J., Maryniak, M., Narkiewicz, U., Kucharewicz, I., & Wrobel, R. (2005). FMR study of agglomerated nanoparticles in a Fe_3C/C system. *Materials Science-Poland*, *23*, 1001–1008.
34. Helminiak, A., Arabczyk, W., Zolnierkiewicz, G., Guskos, N., & Typek, J. (2011). FMR study of the influence of carburization levels by methane decom-

position on nanocrystalline iron. *Rev. Adv. Mater. Sci*., *29*, 166–174.

35. Kliava, J. (2009). Electron magnetic resonance of nanoparticles: Superparamagnetic resonance. In S. P. Gubin (Ed.), *Magnetic nanoparticles* (pp. 255–302). Wiley-VCH. Retrieved 15 September 2009, from http://onlinelibrary.wiley.com/book/10.1002/9783527627561.